DFT-Based Channel Estimation and Noise Variance Estimation Techniques for Single-Carrier FDMA

Gillian Huang, Andrew Nix and Simon Armour
Centre for Communications Research, University of Bristol
Merchant Venturers Building, Woodland Road, Bristol BS8 1UB, UK
Email: {G.Huang, Andy.Nix, Simon.Armour}@bristol.ac.uk

***Abstract*—Practical frequency domain equalization (FDE) systems generally require knowledge of the channel and the noise variance to equalize the received signal in a frequency-selective fading channel. Accurate channel estimate and noise variance estimate are thus desirable to improve receiver performance. In this paper we investigate the performance of the denoise channel estimator and the approximate linear minimum mean square error (A-LMMSE) channel estimator with channel power delay profile (PDP) mismatch and noise variance estimation errors for a single carrier frequency division multiple access (SC-FDMA) system. A windowed DFT-based noise variance estimator is also presented in this paper to improve A-LMMSE channel estimation as well as to facilitate the MMSE-FDE design. Results show that the proposed noise variance estimator remains unbiased up to a SNR of 50dB.**

I. Introduction

Single carrier frequency division multiple access (SC-FDMA) is employed in the 3GPP long-term evolution (LTE) uplink standard [1] because of its low peak-to-average power ratio (PAPR) [2]. Currently, practical LTE uplink schemes are based on SC-FDMA with localized subcarrier mapping; i.e. localized FDMA (LFDMA). In contrast to the scattered pilot pattern used in the orthogonal frequency division multiple access (OFDMA) based LTE downlink, the LTE uplink specifies a block where all the subcarriers in a SC-FDMA symbol are pilots [1]. Although SC-FDMA has attracted considerable research interest, the area of channel estimation and noise variance estimation for LFDMA is not well addressed in the literature.

Various DFT-based channel estimators have been proposed for orthogonal frequency division multiplexing (OFDM). The least squares (LS) channel estimator is commonly used in practice, but it suffers from an approximate 3dB performance loss compared to the optimal linear minimum mean square error (LMMSE) channel estimator [3]. A denoise estimator can reduce the estimation noise at low signal-to-noise ratios (SNR) but exhibits an error floor at high SNR [3]. The LMMSE channel estimator proposed in [4] is robust to channel correlation mismatch. However, unlike the efficient fast Fourier transform (FFT) algorithm, the Karhuen-Loeve transform (KLT) in [4] results in considerable practical complexity. The approximate LMMSE (A-LMMSE) estimator in [5] gives a good trade-off between complexity and performance. Since this previous research assumes ideal knowledge of the channel power delay profile (PDP) and noise variance, the impact of both mismatches on the performance of the practical A-LMMSE channel estimator is investigated in this paper.

The SC-FDMA receiver also requires a noise variance estimator for MMSE frequency domain equalization (FDE) (and A-LMMSE channel estimation). The DFT-based low rank noise variance estimator reported in [6] is biased at high SNR due to the residual channel power. In [7] virtual subcarriers are used to estimate the noise variance in OFDM systems. When applying this concept to SC-FDMA systems, the noise variance can be estimated using the unoccupied frequency resource or guard subcarriers. However, different frequency resources may experience different levels of interference, which is considered as part of the received noise. It is more desirable to estimate the user in-band noise variance. The KLT-based noise variance estimator [8] gives a good in-band noise variance estimation performance, but again the complexity of the KLT is high. In this paper, we present a novel windowed DFT-based noise variance estimator that is able to estimate the user in-band noise variance with negligible bias.

This paper focuses on low complexity DFT-based estimation techniques for SC-FDMA. The paper is organized as follows. Section II describes the SC-FDMA system and the equivalent channel. In Section III, the denoise and A-LMMSE channel estimators are discussed. In Section IV, the windowed DFT-based noise variance estimation technique is described. The performance of the channel estimation and noise variance estimation techniques is presented in Section V. Section VI concludes the paper.

II. System and Channel Description

The block diagram of an SC-FDMA system is shown in Fig. 1. x_m denotes the baseband transmit symbols, where $m = 0, \ldots, M-1$. M is the number of user subcarriers. x_m is converted to the frequency domain (FD) via an M-point discrete Fourier transform (DFT). The FD symbols are then mapped onto a group of localized subcarriers (i.e. LFDMA) and converted back to the time domain (TD) via an N-point inverse DFT (IDFT), where N represents the total number of available subcarriers. Finally, a cyclic prefix (CP) is inserted to construct an SC-FDMA transmission block.

The receiver performs the inverse process. The FDE block is omitted in Fig. 1. Let g_l denote the equivalent channel impulse response (CIR) after localized subcarrier demapping, where $l = 0, \ldots, M-1$. Since the CP makes the linear convolution of

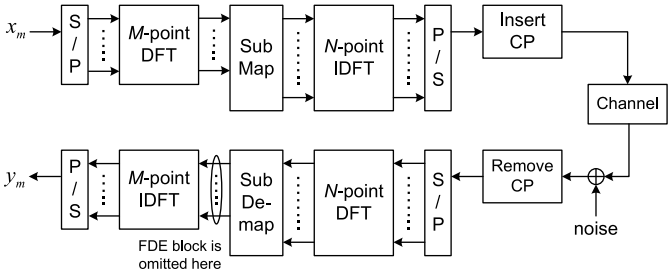

Fig. 1. Block diagram of an SC-FDMA system

the channel appear to be cyclic at the receiver, the unequalized baseband symbols in the TD can be described as [9]

$$y_m = g_l \otimes x_{m-l} + \eta_m, \quad m = 0, \ldots, M-1 \tag{1}$$

where $\otimes$ denotes cyclic convolution and η_m is the equivalent received noise. The cyclic convolution of the channel and the transmit symbols is equivalent to FD multiplication. This facilitates the use of an efficient one-tap per subcarrier FDE. The commonly used MMSE-FDE is described as

$$q_k = \frac{h_k^*}{|h_k|^2 + \sigma_n^2}, \quad k = 0, \ldots, M-1 \tag{2}$$

where h_k is the (estimated) channel response on the k-th subcarrier and σ_n^2 is the (estimated) received noise variance.

Note: Since the DFT assumes a periodic extension, the discontinuities at the frequency edges of h_k give rise to an energy smearing effect to g_l. Hence the channel energy of g_l is smeared over all the taps and most of the channel energy is concentrated in just a few taps [3]. This energy smearing effect is important to the DFT-based estimator design.

III. DFT-Based Channel Estimation

A generic DFT-based channel estimator is described as follows. Let s_k denote the transmit pilot symbols on the k-th subcarrier, the received pilot symbols can be described as

$$r_k = h_k s_k + n_k \tag{3}$$

where n_k is the received noise.

Fig. 2 shows a DFT-based channel estimator architecture. The transmit pilot symbols are assumed to have unity power, $|s_k|^2 = 1$, e.g. a Chu sequence [10]. The initial LS channel estimate can be obtained as

$$\hat{h}_{\mathrm{LS},k} = s_k^* r_k = h_k + \varepsilon_k \tag{4}$$

where $\varepsilon_k = s_k^* n_k$ denotes the FD LS estimation noise and $E[|\varepsilon_k|^2] = E[|n_k|^2] = \sigma_n^2$ is the same as the received noise variance. The LS CIR estimate is obtained using an IDFT, i.e.

$$\hat{g}_{\mathrm{LS},l} = \frac{1}{\sqrt{M}} \sum_{k=0}^{M-1} \hat{h}_{\mathrm{LS},k} e^{j\frac{2\pi}{M}kl} = g_l + e_l \tag{5}$$

where e_l is the LS estimation noise in the TD and $E[|e_l|^2] = E[|\varepsilon_k|^2] = \sigma_n^2$.

Assuming ε_k in (4) is uncorrelated Gaussian noise, e_l in (5) will be spread equally all over taps. Since the channel energy

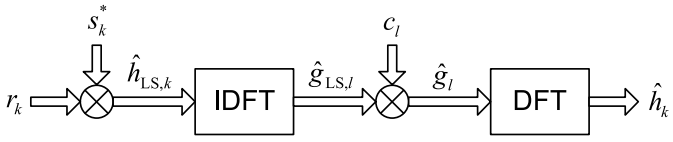

Fig. 2. Block diagram of a DFT-based channel estimator

is concentrated in just a few taps, a scalar filter c_l can be applied to suppress the noise and improve the accuracy of the channel estimate. The filtered CIR estimate is described as

$$\hat{g}_l = c_l \hat{g}_{\mathrm{LS},l}. \tag{6}$$

Finally, $\hat{g}_l$ is converted back to the FD, i.e. $\hat{h}_k = \frac{1}{\sqrt{M}} \sum_{l=0}^{M-1} \hat{g}_l e^{-j\frac{2\pi}{M}kl}$. The filtered channel estimate $\hat{h}_k$ is then used in (2) to obtain the MMSE-FDE coefficients.

The DFT-based denoise channel estimator is revisited in this section since the analysis is closely related to the design of the proposed noise variance estimator. As the LMMSE channel estimator proposed in [4] is not DFT-based, it is not considered further in this paper.

A. Denoise Channel Estimator

The denoise estimator assumes that the channel energy in the smearing region is zero and hence these taps contain only noise. The denoise estimator is described as

$$c_l = \begin{cases} 1, & l \notin A \\ 0, & l \in A \end{cases} \tag{7}$$

where $A = \{l : L+S, \ldots, M-S-1\}$ is defined as the channel energy smearing region and $l \notin A$ is defined as the energy concentration region. L can be the equivalent maximum channel delay spread or the equivalent CP length normalized to the user symbol rate. S denotes the number of taps that have significant smearing energy to be excluded from the denoising processing. The choice of S is investigated in [3], and there is a tradeoff between better noise reduction and a lower estimation error floor.

The truncation of the channel energy smearing taps leads to an estimation error floor at high SNR. The resultant estimation bias in the FD is analyzed as follows. Let β_i denote the DFT of c_l (e.g. β_i is a sinc filter since the denoise estimator coefficients form a rectangular window). β_i can be seen as a low pass filter that smooths the FD channel response and removes the high-frequency noise components. Since the multiplication in (6) gives a cyclic convolution in the FD, the resultant channel estimate $\hat{h}_k$ can be expressed as

$$\hat{h}_k = \beta_i \otimes \hat{h}_{\mathrm{LS},k-i} = \underbrace{\beta_i \otimes h_{k-i}}_{\text{distorted channel}} + \underbrace{\beta_i \otimes \varepsilon_{k-i}}_{\text{filtered noise}}. \tag{8}$$

In (8), although the noise $\beta_i \otimes \varepsilon_{k-i}$ is reduced by the cyclic filtering, the true channel response is distorted. Let $\beta_i \otimes h_{k-i} = h_k + b_k$, where b_k denotes the channel distortion on the k-th subcarrier. Note that the channel response can be highly uncorrelated from one edge of the frequency band to the other but β_i smooths the channel response cyclically. As

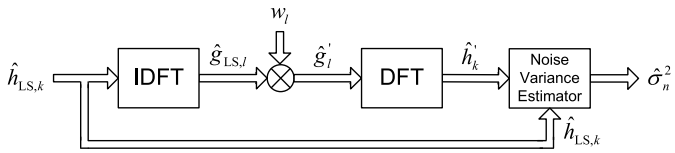

Fig. 3. Windowed DFT-based noise variance estimator

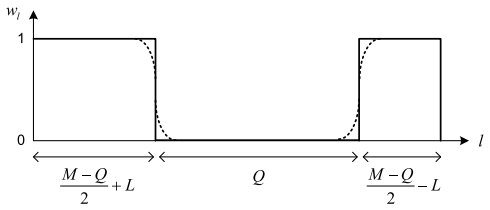

Fig. 4. The time-domain window function. The solid line denotes a rectangular window, and the dotted line denotes a window with a smooth transition band.

a result, large channel distortion b_k occurs at the frequency edges. Moving towards the middle of the frequency band, the channel response on adjacent subcarriers are more correlated, hence the channel distortion b_k is small. In other words, the estimation bias of the denoise estimator is not distributed uniformly across all subcarriers.

B. A-LMMSE Channel Estimator

The A-LMMSE channel estimator provides a lower complexity than the LMMSE channel estimator by ignoring the channel correlation between the TD taps. Hence the aim is to minimize the MSE of the filtered channel estimate on each tap independently. The MSE on the l-th tap can be written as

$$J_l = E\left[\left|c_l\hat{g}_{\mathrm{LS},l} - g_l\right|^2\right]. \tag{9}$$

By taking the derivative of J_l with respect to c_l and equating it to zero (i.e. $\frac{dJ_l}{dc_l} = 0$), the A-LMMSE channel estimator coefficients are obtained as

$$c_l = \frac{\gamma_l}{\gamma_l + \sigma_n^2} \tag{10}$$

where $\gamma_l = E[|g_l|^2]$ is the expected channel PDP.

In (10), knowledge of the channel PDP and the noise variance is required to calculate the A-LMMSE channel estimator coefficients. Although the average channel PDP can be acquired via real-time tracking, it is difficult to obtain an accurate channel PDP in the highly mobility scenario and in the frequency hopping (FH) mode, where the channel statistics change rapidly. It is shown in [4] that the LMMSE channel estimator is robust to channel correlation mismatch when a rectangular PDP is assumed. Hence the rectangular channel PDP is assumed in this paper for practical A-LMMSE design. The noise variance estimation technique is described in the following section.

IV. Windowed DFT-Based Noise Variance Estimation Technique

The DFT-based noise variance estimator reported in [6] uses the same assumption as the denoise channel estimator, i.e. all the taps outside the energy concentration region contain noise only. Hence this low rank noise variance estimator is described as

$$\hat{\sigma}_n^2 = \frac{1}{\text{length}\,(A)}\sum_{l\in A}\left|\hat{g}_{\mathrm{LS},l}\right|^2. \tag{11}$$

Since non-negligible g_l remains in the energy smearing region, this approach gives significant bias at high SNR. In this section, we present a windowed DFT-based noise variance estimation technique that gives negligible bias.

Fig. 3 shows the block diagram of the proposed noise variance estimator. A window function w_l is applied to $\hat{g}_{\mathrm{LS},l}$ prior to converting it back to the FD. The windowed channel estimate $\hat{h}_k'$ is then used in conjunction with the LS channel estimate $\hat{h}_{\mathrm{LS},k}$ to estimate the noise variance.

The TD window function w_l is illustrated in Fig. 4, where Q denotes the number of samples in the stopband. w_l is offset by L samples as the first L taps contain most of channel energy. The TD channel estimate after windowing can be written as

$$\hat{g}_l' = w_l\hat{g}_{\mathrm{LS},l} = g_l' + e_{\mathrm{R},l} \tag{12}$$

where $g_l' = w_l g_l$ is the channel response after windowing and $e_{\mathrm{R},l} = w_l e_l$ is the remaining noise after windowing.

After converting $\hat{g}_l'$ back to the FD, the remaining noise in the FD is described as $\varepsilon_{\mathrm{R},k} = \frac{1}{\sqrt{M}}\sum_{l=0}^{M-1} w_l e_l e^{-j\frac{2\pi}{M}kl}$. Assuming that e_l is white Gaussian noise, $\varepsilon_{\mathrm{R},k}$ will be Gaussian noise that is slightly correlated in the FD due to the windowing. Hence the FD LS estimation noise can be written as

$$\varepsilon_k = \varepsilon_{\mathrm{R},k} + \varepsilon_{\mathrm{E},k} \tag{13}$$

where $\varepsilon_{\mathrm{E},k}$ denotes the FD estimation noise that is to be eliminated by the TD windowing process.

Let a_j denote the DFT of w_l (e.g. a_j is a sinc function when w_l is a rectangular window). Since the multiplication $g_l' = w_l g_l$ results in cyclic convolution in the FD, the windowed FD channel (without noise) can be expressed as

$$h_k' = a_j \otimes h_{k-j} = h_k + d_k \tag{14}$$

where d_k denotes the resultant FD channel distortion due to windowing. As mentioned in Section III (A), a_j can be perceived as a low-pass filter that smooths the FD channel response cyclically. Hence the channel distortion d_k is large on the subcarriers at the frequency edges, and d_k becomes smaller as we move towards the center of the frequency band.

Based on the above analysis, the LS channel estimate and the windowed channel estimate can be expressed as (15) and (16) respectively.

$$\hat{h}_{\mathrm{LS},k} = h_k + \varepsilon_k = h_k + \varepsilon_{\mathrm{R},k} + \varepsilon_{\mathrm{E},k} \tag{15}$$

$$\hat{h}_k' = h_k' + \varepsilon_{\mathrm{R},k} = h_k + d_k + \varepsilon_{\mathrm{R},k} \tag{16}$$

By taking the average squared difference of $\hat{h}_{\mathrm{LS},k}$ and $\hat{h}_k'$ in the frequency range where d_k is negligible, we can estimate the variance of $\varepsilon_{\mathrm{E},k}$ (denoted as $\sigma_{\mathrm{E}}^2 = E[|\varepsilon_{\mathrm{E},k}|^2]$). Since the

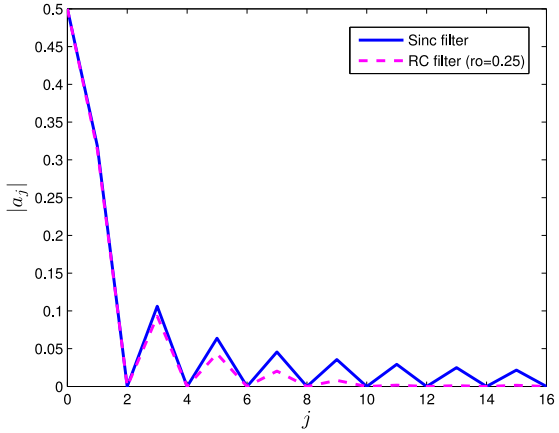

Fig. 5. Filter response with rectangular window and RC window

mean ratio of σ_n^2 to σ_{E}^2 is $\frac{M}{Q}$, the received noise variance can be estimated as

$$\hat{\sigma}_n^2 = \frac{M}{Q}.\hat{\sigma}_{\mathrm{E}}^2 = \frac{M}{Q}.\frac{1}{M-2K}\sum_{k=K}^{M-K-1}\left|\hat{h}_{\mathrm{LS},k} - \hat{h}'_k\right|^2 \quad (17)$$

where K is specified as the number of subcarriers at the frequency edges that contain large d_k.

Choice of Parameters: There is a compromise when choosing the number of stopband samples Q. Large Q (equivalent to a small passband) gives a wider mainlobe and sidelobes to the FD smoothing filter a_j. In this case, larger K has to be chosen to ensure $d_k \approx 0$. Less available samples in the averaging region lowers the accuracy of the estimate $\hat{\sigma}_{\mathrm{E}}^2$. As a result, the accuracy of $\hat{\sigma}_n^2$ is reduced. If a small value of Q is used, the instantaneous ratio of σ_n^2 to σ_{E}^2 may deviate considerably from its mean ratio $\frac{M}{Q}$. This also lowers the accuracy of $\hat{\sigma}_n^2$. Hence, as a compromise, $Q = \frac{M}{2}$ is used in this paper.

For a rectangular w_l, a_j is a sinc filter and its sidelobes roll off slowly. This makes the channel distortion d_k roll off slowly in the FD. Therefore, the noise variance estimate can be slightly biased at high SNR when d_k is large compared to $\varepsilon_{\mathrm{E},k}$. As an improvement to the proposed noise variance estimation technique, a window function with a smooth transition band (as shown in Fig. 4) can be applied to reduce the sidelobes of a_j. Using this approach the estimation bias problem at high SNR can be further improved.

Fig. 5 shows the filter response a_j with a rectangular window and a raised cosine (RC) window, where $M = 128$ and $Q = \frac{M}{2} = 64$. It is shown that a RC filter with a small rolloff factor of 0.25 has much lower sidelobes than a sinc filter. After four sidelobes (e.g. $K = 11$ samples), $a_j \approx 0$.

V. Results and Discussion

In the simulation for an LFDMA system, the total number of available subcarriers N is 512 and the number of user subcarriers M is 128. The subcarrier spacing is 15kHz [1] and the sample period is $T_s = \frac{1}{15\mathrm{kHz}\times 512} = 0.1302\mu s$. The CP length is set to $P = 36$ (i.e. $4.69\mu s$). The urban macro scenario of the spatial channel model extended (SCME) [11] is used, and the CP length is thus longer than the maximum channel delay spread of $4.60\mu s$. The baseband modulation scheme is QPSK. The pilot symbols are based on a Chu sequence [10]. For the denoise channel estimators, the number of significant energy smearing taps is set to $S = 5$ as a compromise between noise reduction and estimation bias [3]. The equivalent CP length is $L = P \times \frac{M}{N} = 9$. For the windowed noise variance estimator, $K = 11$ is used. The ideal A-LMMSE channel estimator is used as a lower bound.

Fig. 6 shows the performance comparison of the DFT-based noise variance estimators. As the low rank noise variance estimator gives a large bias at high SNR, the proposed noise variance estimator gives a much lower bias. When a RC window with a small rolloff factor of 0.25 is used, no bias is observed up to SNR $= 50$dB.

Fig. 7 shows the MSE of the A-LMMSE channel estimator with mismatches, where a rectangular channel PDP is assumed. When prefect noise variance is used, the A-LMMSE gives some degradation due to PDP mismatch at low SNR. However, at high SNR it is robust to the PDP mismatch. When taking the noise variance estimation error into account, it can be seen that the A-LMMSE is sensitive to noise variance estimation bias. As the proposed noise variance estimator (with RC window) gives negligible bias, no performance degradation of the A-LMMSE due to noise variance estimation error is observed in Fig. 7. Hence a robust A-LMMSE can be designed with the rectangular channel PDP and the proposed noise variance estimator. For the following results, the RC windowed noise variance estimator is assumed for A-LMMSE and MMSE-FDE coefficient calculation.

Fig. 8 shows the MSE comparison of the DFT-based channel estimators. As expected, the denoise channel estimator gives an error floor at high SNR due to the truncation of the channel energy. The practical A-LMMSE approach (with mismatches) has similar performance to the ideal A-LMMSE. Both achieve good noise reduction at low SNR and converge to the LS estimator at high SNR.

Fig. 9 shows the BER of LFDMA with different DFT-based channel estimators. While the LS channel estimator gives approximately 3dB of performance loss compared to the ideal-LMMSE estimator, the practical A-LMMSE can provide an improved performance (i.e. within 1.5dB of the ideal-LMMSE at a BER of 0.001). Note that the denoise channel estimator shows an increased BER at high SNR while the MSE is flat. This is because as the estimation error b_k persists and the estimated noise variance $\hat{\sigma}_n^2$ reduces, the impact of b_k on the MMSE-FDE coefficient error becomes larger at high SNR (see eq. (2)). This results in larger equalization error, and hence an increased BER, at high SNR.

VI. Conclusions

In this paper, the performance of a practical A-LMMSE channel estimator with channel PDP mismatch and noise variance estimation error is investigated. Results show that the performance of the A-LMMSE is fairly robust to channel

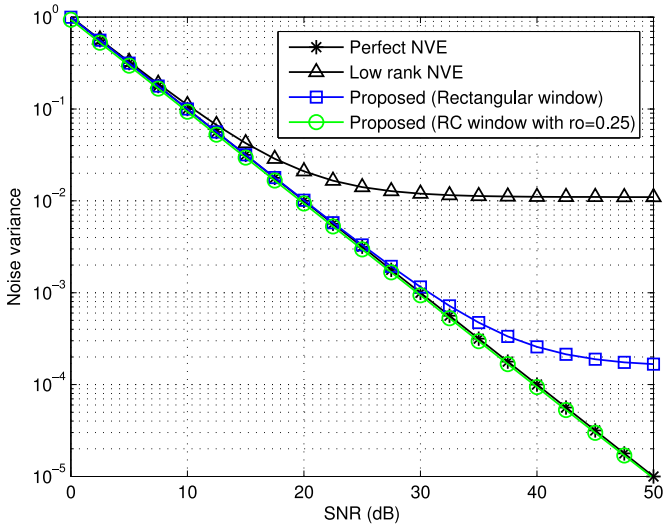

Fig. 6. Performance comparison of DFT-based noise variance estimators

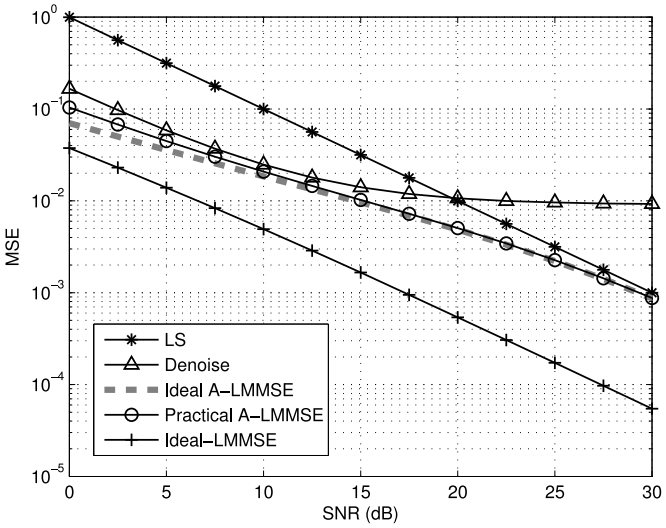

Fig. 8. MSE comparison of DFT-based channel estimators

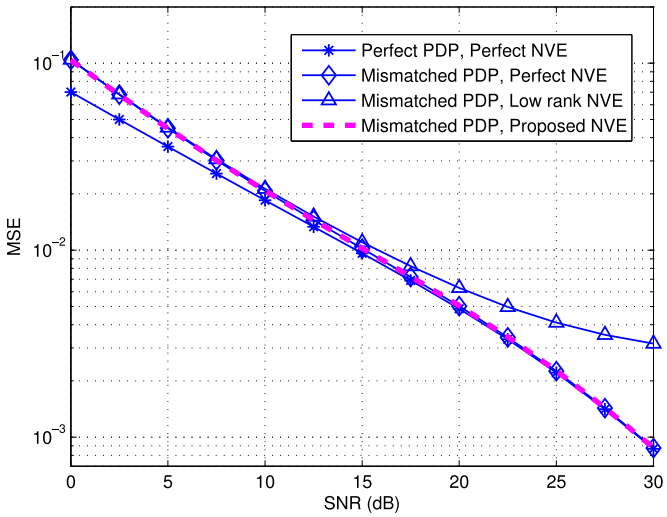

Fig. 7. MSE of the A-LMMSE channel estimator with channel PDP mismatch and noise variance estimation error

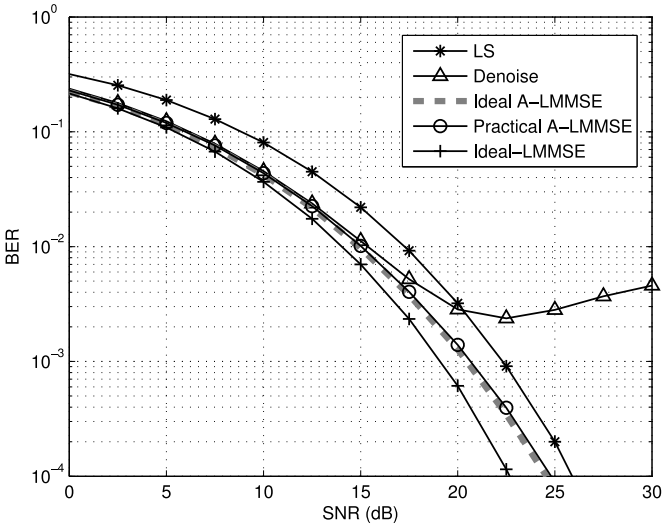

Fig. 9. BER of LFDMA with different DFT-based channel estimators

PDP mismatch when a rectangular channel PDP is assumed. However, the performance of the A-LMMSE is shown to be sensitive to noise variance estimation bias. The paper also proposes a windowed noise variance estimation technique with negligible bias to facilitate the design of MMSE-FDE and to improve the performance of the practical A-LMMSE channel estimator.

REFERENCES

[1] 3GPP TS 36.211, "Evolved universal terrestrial radio access (E-UTRA); Physical channel and modulation (Release 8)," Dec. 2008. http://www.3gpp.org/ftp/Specs/html-info/36212.htm.

[2] H. Myung, J. Lim, and D. Goodman, "Single carrier FDMA for uplink wireless transmission," *IEEE Veh. Tech. Mag.*, vol. 1, pp. 30-38, Sept. 2006.

[3] J. J. van de Beek, O. Edfors, M. Sandell, S. K. Wilson, and P. O. Borjesson, "On channel estimation in OFDMA systems," in *Proc. VTC'95-Spring*, vol. 2, pp. 815-819, Jul. 1995

[4] O. Edfors, M. Sandell, J. J. van de Beek, S. K. Wilson, and P. O. Borjesson, "OFDM channel estimation by singular value decomposition," *IEEE Trans. Commun.*, vol. 46, pp. 931-939, Jul. 1998.

[5] O. Edfors, M. Sandell, J. J. van de Beek, S. K. Wilson, and P. O. Borjesson, "Analysis of DFT-based channel estimators for OFDM," *Wireless Personal Commun.*, vol. 12, no. 1, pp. 55-70, Jan. 2000.

[6] Y. Zheng and C. Xiao, "Frequency-domain channel estimation and equalization for broadband wireless communications," in *Proc. ICC'07*, pp. 4475-4480, Jun. 2007.

[7] L. Huang, G. Mathew, and J. Bergmans, "Pilot-aided channel estimation for systems with virtual carriers," in *Proc. ICC'06*, vol. 7, pp. 3070-3075, Jun. 2006.

[8] S. Schiffermuller and V. Jungnickel, "Practical channel interpolation for OFDMA," in *Proc. Globecom'06*, pp. 1-6, Nov. 2006.

[9] G. Huang, A. Nix, and S. Armour, "Decision feedback equalization in SC-FDMA," in *Proc. PIMRC'08*, Sept. 2008.

[10] D. Chu, "Polyphase codes with good periodic correlation properties," *IEEE Trans. Inform. Theory*, vol. 18, no. 4, pp. 531-532, Jul. 1972.

[11] D. Baum, *et al.*, "An interim channel model for beyond-3G system: extending the 3GPP spatial channel model," in *Proc. VTC'05-Spring*, vol. 5, pp. 3132-3136, May 2005.